J. Nonlinear Var. Anal. 7 (2023), No. 6, pp. 909-923
Available online at http://jnva.biemdas.com
https://doi.org/10.23952/jnva.7.2023.6.02

A MODIFIED INVERSE-FREE DYNAMICAL SYSTEM FOR ABSOLUTE VALUE EQUATIONS

XIN HAN[1,2], XING HE[1,*], JIAWEI CHEN[3], XINGXING JU[4]

[1]*Chongqing Key Laboratory of Nonlinear Circuits and Intelligent Information Processing, School of Electronic and Information Engineering, Southwest University, Chongqing, China*
[2]*College of Mathematics, Sichuan University of Arts and Science, Dazhou, China*
[3]*School of Mathematics and Statistics, Southwest University, Chongqing, China*
[4]*College of Electronics and Information Engineering, Sichuan University, Chengdu, China*

Abstract. This paper proposes a novel inverse-free dynamical system for tackling absolute value equations. The proposed dynamical system is an extension of the inverse-free dynamical system designed by Chen et al. (Appl. Numer. Math. 168 (2021), 170-181). A new global error bound for absolute value equation is obtained, which is more compact than the existing ones. The equilibrium point of the proposed dynamical system is proved to be the solution to the corresponding absolute value equation. In contrast to some existing dynamical systems, the distinctive feature of our dynamical system is its simple structure, inverse-free operation, and global sublinear and exponential convergence. Finally, numerical results are provided to demonstrate the effectiveness of our dynamical system.

Keywords. Absolute value equations; Modified inverse-free dynamical system; Global error bound; Sublinear convergence; Exponential convergence.

1. Introduction

In this paper, we consider the absolute value equation (AVE), which is formulated as follows:

$$\boldsymbol{A}\boldsymbol{y} - \left|\boldsymbol{y}\right| - \boldsymbol{b} = \boldsymbol{0}, \tag{1.1}$$

where $\boldsymbol{A} \in \mathbb{R}^{m\times m}$, $\boldsymbol{y} \in \mathbb{R}^m$, $\boldsymbol{b} \in \mathbb{R}^m$, and $\left|\boldsymbol{y}\right| \in \mathbb{R}^m$ represents the component-wise absolute value of $\boldsymbol{y}$ whose the k-th component is y_k if $y_k \in \mathbb{R}_+ \cup \left\{0\right\}$ and $-y_k$ otherwise. It is worth pointing out that AVE (1.1) is NP-hard [1] owing to its non-differentiability and nonlinearity. In recent years, AVE (1.1) has attracted much attention, mainly since it is related to many scientific computing and engineering problems, such as variational inequality (VI) problems, interval linear equations, mixed integer programming problems, linear complementarity problems (LCP), economic equilibrium problems, and others; see, e.g., [1–7] and references therein.

To analyze theoretical properties and effectively solve the AVE, many sufficiency conditions on solvability and numerical calculation methods were studied in [1, 5, 7–12]. As described

*Corresponding author.
E-mail address: hanmath@163.com (X. Han), hexingdoc@swu.edu.cn (X. He), j.w.chen713@163.com (J. Chen), xingxju@scu.edu.cn (X. Ju).

Received March 21, 2023; Accepted June 27, 2023.

in [1], the general NP-hard LCP subsuming many nonlinear optimization problems can be equivalent to an AVE. Nonetheless, by means of the connection between LCP and the AVE, it was proved in [1] that the AVE has a unique solution if the least singular value of the coefficient matrix is strictly greater than one. Moreover, when the coefficient matrix has some specific forms, the authors in [7] demonstrated the unique solvability of the AVE. In recent years, many numerical methods have been investigated for the AVE. For instance, the generalized Newton method was studied in [9] and then its modified version was devised in [10]. Moreover, the authors in [11] proposed a SOR-like iteration method, and then its modified version was developed in [12].

It is worth noticing that the numerical methods mentioned above to solve the AVE are all discrete, and they usually need to coordinate the iteration step length and search direction to realize the fast computation goal. Compared with these discrete methods, it is known that dynamical systems have the advantages of acquisition of real-time solutions, parallel processing of information and induction of some possible discrete methods; see, e.g., [13–16]. In the last decades, from the perspective of neurodynamic algorithms, many dynamical systems (see [14, 15, 17–20] and the references therein) have been widely used to tackle various problems. However, few researchers devised dynamical systems to seek the solution to the AVE. This article focuses on the dynamical systems for solving the AVE. To find the exact solution, the globally convergent double-projection dynamical system was proposed in [19], and the asymptotically stable projection dynamical system was constructed in [20]. In [21], the AVE was equivalently transformed into a differentiable unconstrained problem with the aid of smooth approximation technique. Then, the unified smoothing dynamical system was devised for tackling the differentiable unconstrained problem. Recently, the authors in [22] reformulated AVE (1.1) as an LCP, and devised a projection-based dynamical system to address this LCP. It is known that the dynamical systems mentioned above for tackling the AVE almost all involve the inverse operation of a matrix or some matrices, which may lead to a large amount of calculation, especially for the high-dimensional AVE problems. To overcome this limitation and directly tackle the AVE, the authors in [23] proposed an asymptotically stable inverse-free dynamical system without involving any matrix inversion operation. More recently, to inherit the inverse-free advantage stated in [23], the authors in [24] devised an inertial inverse-free dynamical system by introducing an inertial term. Compared with the dynamical system with single-layer structure in [23], although the dynamical system in [24] enjoys the acceleration characteristics, it is a two-layer structure and involves more neurons, which will increase the hardware consumption [25]. Considering that the inverse-free dynamical system in [23] is not only simple in structure but also does not involve any matrix inversion operation, it is necessary to study the inverse-free dynamical system with concise structure to address the AVE quickly.

Motivated by the work in [23], we propose a novel inverse-free dynamical system. If the designed parameters satisfy certain conditions, the proposed dynamical system reduces to the dynamical system in [23]. Furthermore, the reduced dynamical system is proved to be globally exponentially convergent. Compared with the error bound involved in [23], a tighter global error bound for AVE (1.1) is obtained. By virtue of the global error bound, the global sublinear and exponential convergence of the proposed dynamical system are established under some suitable conditions on the designed parameters. Detailed comparisons of our dynamical system with the dynamical system in [23] are given by a numerical example. It can be observed from the simulation results that our dynamical system is effective and has certain advantages in tackling the AVE.

The rest of this work is organized as below. Section 2 introduces some preliminaries for the AVE. Section 3 proposes a novel inverse-free dynamical system and presents a new global error bound for the AVE. Convergence results are presented in Section 4. Numerical simulation results are presented in Section 5. The last section, Section 6 concludes this work.

2. Preliminaries

2.1. **Notations.** Let $\mathbb{R}_+$ be the set of positive real numbers. Let $\boldsymbol{0}$ stand for a column vector with all entries being $0 \in \mathbb{R}$ (its size is to be understood from this paper). $\boldsymbol{E}_m$ denotes the m-order identity matrix. $(\cdot)^\top$ denotes the transpose. $\langle \cdot, \cdot \rangle$ denotes the inner product. For the matrix $\boldsymbol{B}$, the spectral norm is denoted by $\|\boldsymbol{B}\|_2$. Moreover, denote $\|\cdot\|_1$ and $\|\cdot\|$ as the ℓ_1-norm and ℓ_2-norm, respectively. For $p \in \mathbb{R}_+$ and $\boldsymbol{y} \in \mathbb{R}^m$, we set $\|\boldsymbol{y}\|_p = \left(\sum_{i=1}^m |y_i|^p\right)^{\frac{1}{p}}$. Denote $|\cdot|$ as the absolute value vectors (matrices) defined by $|\boldsymbol{b}| = \left(|b_1|, \cdots, |b_m|\right)^\top$ ($|\boldsymbol{B}| = \left(|b_{ij}|\right)_{mm}$). $\text{Eigvals}(\boldsymbol{B})$ and $\text{Eigvecs}(\boldsymbol{B})$ denote the eigenvalues and eigenvectors space of the matrix $\boldsymbol{B}$, respectively. Let $\lambda_{\min}(\boldsymbol{B})$ denote the smallest eigenvalue of the matrix $\boldsymbol{B}$. Denote $\text{tridiag}(c, d, e)$ as a matrix whose the sub-diagonal, the main diagonal, the super-diagonal and other entries are $c \in \mathbb{R}$, $d \in \mathbb{R}$, $e \in \mathbb{R}$ and $0 \in \mathbb{R}$, respectively. $0 < \boldsymbol{D} \in \mathbb{R}^{m\times m}$ means that the matrix $\boldsymbol{D}$ is positive definite.

2.2. **Problem formulation.** Let $\Theta(\boldsymbol{y}) \triangleq (\boldsymbol{A}+\boldsymbol{E})\boldsymbol{y} - \boldsymbol{b}$, $\Xi(\boldsymbol{y}) \triangleq (\boldsymbol{A}-\boldsymbol{E})\boldsymbol{y} - \boldsymbol{b}$ and $\Omega \triangleq \left\{\boldsymbol{y} : \boldsymbol{0} \le \boldsymbol{y} \in \mathbb{R}^m\right\}$. According to the analysis of [1, 23], it can be known that the AVE (1.1) is equivalent to the following general LCP: find a $\boldsymbol{y} \in \mathbb{R}^m$ such that

$$\Theta(\boldsymbol{y}) \ge 0,\ \Xi(\boldsymbol{y}) \ge 0 \text{ and } \left\langle \Theta(\boldsymbol{y}), \Xi(\boldsymbol{y}) \right\rangle = 0. \tag{2.1}$$

Note that (2.1) is a special case of the following VI: find a $\boldsymbol{y} \in \mathbb{R}^m$ such that $\Theta(\boldsymbol{y}) \in \Omega$ and

$$\left\langle \boldsymbol{x} - \Theta(\boldsymbol{y}), \Xi(\boldsymbol{y}) \right\rangle \ge 0,\ \forall \boldsymbol{x} \in \Omega, \tag{2.2}$$

which is equivalent to the projection equation [6]:

$$\Theta(\boldsymbol{y}) = P_\Omega\left[\Theta(\boldsymbol{y}) - \Xi(\boldsymbol{y})\right], \tag{2.3}$$

where $P_\Omega(\cdot)$ denotes the projection operator, and $P_\Omega(\boldsymbol{z}) \triangleq \arg\min_{\boldsymbol{y}\in\Omega} \|\boldsymbol{y} - \boldsymbol{z}\|$ for all $\boldsymbol{z} \in \mathbb{R}^m$.

Before proceeding, the following assumption is adopted for our analysis.

Assumption 2.1. For $\boldsymbol{A} \in \mathbb{R}^{m\times m}$ in AVE (1.1), $\lambda_{\min}(\boldsymbol{A}^\top \boldsymbol{A}) > 1$, i.e., $\sigma_{\min}(\boldsymbol{A}) > 1$, where $\sigma_{\min}(\boldsymbol{A})$ stands for the least singular value of the m-order matrix $\boldsymbol{A}$.

Remark 2.1. Assumption 2.1 has received extensive attention (see, e.g., [1, 7, 8, 23]). From [1, Proposition 3], it follows that Assumption 2.1 is given to ensure that AVE (1.1) has a unique solution. Moreover, Assumption 2.1 indicates that it makes sense to devise some computing methods to tackle AVE (1.1).

2.3. **Definitions and technical lemmas.** Consider the following dynamical system

$$\begin{cases} \dot{\boldsymbol{y}}(t) = \mathscr{F}\big(\boldsymbol{y}(t)\big), \\ \boldsymbol{y}\big(t_0\big) = \boldsymbol{y}_0 \in \mathbb{R}^m, \end{cases} \tag{2.4}$$

where $\mathscr{F} : \mathbb{R}^m \to \mathbb{R}^m$ is a continuous function.

Definition 2.1. [26] A vector $\boldsymbol{y}^* \in \mathbb{R}^m$ is called an equilibria of system (2.4) if $\mathscr{F}\big(\boldsymbol{y}^*\big) = \boldsymbol{0}$.

Definition 2.2. [26] An equilibrium point $\boldsymbol{y}^* \in \mathbb{R}^m$ of system (2.4) is said to be globally exponentially stable if there exists two positive constants κ and γ such that

$$\big\|\boldsymbol{y}(t) - \boldsymbol{y}^*\big\| \leq \kappa\big\|\boldsymbol{y}_0 - \boldsymbol{y}^*\big\| \exp\big(-\gamma(t-t_0)\big)$$

holds for each solution $\boldsymbol{y}(t) \in \mathbb{R}^m$ with $t \geq t_0$.

Next, we give some basic properties of AVE (1.1).

Lemma 2.1. *[23] Let $\varepsilon(\boldsymbol{y}) \triangleq \Theta(\boldsymbol{y}) - P_\Omega\big[\Theta(\boldsymbol{y}) - \Xi(\boldsymbol{y})\big]$ in (2.3). Then, $\boldsymbol{y}^*$ is a solution to AVE (1.1) iff $\varepsilon\big(\boldsymbol{y}^*\big) = \boldsymbol{0}$. Moreover, $\varepsilon(\boldsymbol{y}) = \boldsymbol{A}\boldsymbol{y} - \big|\boldsymbol{y}\big| - \boldsymbol{b}$ can be obtained directly.*

Lemma 2.2. *[23] For AVE (1.1), if $\sigma_{\min}(\boldsymbol{A}) \in [1, +\infty)$ and $\boldsymbol{y}^* \in \mathbb{R}^m$ is a solution of this equations, then*

$$\Big\langle \boldsymbol{y} - \boldsymbol{y}^*, \boldsymbol{A}^\top\big(\boldsymbol{A}\boldsymbol{y} - |\boldsymbol{y}| - \boldsymbol{b}\big)\Big\rangle \geq \frac{1}{2}\big\|\boldsymbol{A}\boldsymbol{y} - |\boldsymbol{y}| - \boldsymbol{b}\big\|^2,$$

for any $\boldsymbol{y} \in \mathbb{R}^m$.

3. Inverse-Free Dynamical System

Before devising the dynamical system, we establish a new global error bound for AVE (1.1) as follows.

Lemma 3.1. *Let $\Lambda(\boldsymbol{y}) = \boldsymbol{A}\boldsymbol{y} - \big|\boldsymbol{y}\big| - \boldsymbol{b}$. If Assumption 2.1 is satisfied and $\boldsymbol{y}^* \in \mathbb{R}^m$ is the unique solution to AVE (1.1), then*

$$\frac{1}{\kappa_1 + \kappa_2}\big\|\Lambda(\boldsymbol{y})\big\| \leq \big\|\boldsymbol{y} - \boldsymbol{y}^*\big\| \leq \frac{\kappa_1 + \kappa_2}{\delta}\big\|\Lambda(\boldsymbol{y})\big\| \tag{3.1}$$

holds for any $\boldsymbol{y} \in \mathbb{R}^m$, where

$$\kappa_1 \triangleq \begin{cases} \rho\big(\boldsymbol{A} + \boldsymbol{E}_m\big), & \boldsymbol{y} - \boldsymbol{y}^* \in \mathrm{Eigvecs}\big(\boldsymbol{A} + \boldsymbol{E}_m\big), \\ \big\|\boldsymbol{A} + \boldsymbol{E}_m\big\|_2, & \text{otherwise}, \end{cases} \tag{3.2}$$

with $\rho\big(\boldsymbol{A} + \boldsymbol{E}_m\big) \triangleq \max\big\{|\lambda| : \lambda \in \mathrm{Eigvals}\big(\boldsymbol{A} + \boldsymbol{E}_m\big)\big\}$ denoting the spectral radius of $\boldsymbol{A} + \boldsymbol{E}_m$,

$$\kappa_2 \triangleq \begin{cases} \rho\big(\boldsymbol{A} - \boldsymbol{E}_m\big), & \boldsymbol{y} - \boldsymbol{y}^* \in \mathrm{Eigvecs}\big(\boldsymbol{A} - \boldsymbol{E}_m\big), \\ \big\|\boldsymbol{A} - \boldsymbol{E}_m\big\|_2, & \text{otherwise}, \end{cases} \tag{3.3}$$

with $\rho\big(\boldsymbol{A} - \boldsymbol{E}_m\big) \triangleq \max\big\{|\lambda| : \lambda \in \mathrm{Eigvals}\big(\boldsymbol{A} - \boldsymbol{E}_m\big)\big\}$ being the spectral radius of $\boldsymbol{A} - \boldsymbol{E}_m$, and $\delta \triangleq \lambda_{\min}\big(\boldsymbol{A}^\top\boldsymbol{A}\big) - 1$.

Proof. For simplification, we replace $\varepsilon(\boldsymbol{y})$, $\Theta(\boldsymbol{y})$, $\Theta\big(\boldsymbol{y}^*\big)$, $\Xi(\boldsymbol{y})$, and $\Xi\big(\boldsymbol{y}^*\big)$ with ε, Θ, Θ^*, Ξ and Ξ^*, respectively. From VI (2.2) and the proof of [23, Theorem 3.5], it follows that

$$\Big\langle \varepsilon, \big(\Theta - \Theta^*\big) + \big(\Xi - \Xi^*\big)\Big\rangle \geq \big\|\varepsilon\big\|^2 + \big\langle \Theta - \Theta^*, \Xi - \Xi^*\big\rangle. \tag{3.4}$$

Let $\boldsymbol{D} \triangleq \boldsymbol{A}^\top \boldsymbol{A} - \boldsymbol{E}_m$. Using Assumption 2.1 and the fact that $\boldsymbol{D} = \boldsymbol{D}^\top$, we obtain $\boldsymbol{D} > 0$. Then we have

$$\langle \Theta - \Theta^*, \Xi - \Xi^* \rangle = \Big\langle \boldsymbol{y} - \boldsymbol{y}^*, \boldsymbol{D}\big(\boldsymbol{y} - \boldsymbol{y}^*\big) \Big\rangle \geq 0. \tag{3.5}$$

In addition, by [27, Lemma 6], for $0 < \boldsymbol{D} \in \mathbb{R}^{m\times m}$, there is an orthogonal matrix $\boldsymbol{P} \in \mathbb{R}^{m\times m}$, such that

$$\langle \boldsymbol{x}, \boldsymbol{D}\boldsymbol{x} \rangle = \sum_i^m \lambda_i (\boldsymbol{P}\boldsymbol{x})_i^2 \geq \delta \sum_i^m (\boldsymbol{P}\boldsymbol{x})_i^2 = \delta \|\boldsymbol{P}\boldsymbol{x}\|^2 = \delta \langle \boldsymbol{x}, \boldsymbol{P}^\top \boldsymbol{P}\boldsymbol{x} \rangle = \delta \|\boldsymbol{x}\|^2 \tag{3.6}$$

always holds for any vector $\boldsymbol{x} \in \mathbb{R}^m$ (which may not be the eigenvector of $\boldsymbol{D}$), where $\lambda_i \in \mathbb{R}_+ \big(i \in \{1, \cdots, m\}\big)$ is the eigenvalue of $\boldsymbol{D}$ and $\delta \triangleq \lambda_{\min}(\boldsymbol{A}^\top \boldsymbol{A}) - 1 = \lambda_{\min}(\boldsymbol{D})$. It then follows from (3.5) and (3.6) that

$$\langle \Theta - \Theta^*, \Xi - \Xi^* \rangle \geq \delta \|\boldsymbol{y} - \boldsymbol{y}^*\|^2. \tag{3.7}$$

Further, by (3.4) and (3.7), we see that

$$\delta \|\boldsymbol{y} - \boldsymbol{y}^*\|^2 \leq \langle \Theta - \Theta^*, \Xi - \Xi^* \rangle + \|\varepsilon\|^2 \leq \Big\langle \varepsilon, (\Theta - \Theta^*) + (\Xi - \Xi^*) \Big\rangle. \tag{3.8}$$

Applying the Cauchy-Schwarz inequality and the triangle inequality, we obtain from (3.8) that

$$\|\boldsymbol{y} - \boldsymbol{y}^*\|^2 \leq \frac{1}{\delta} \|\varepsilon\| \Big\| (\Theta - \Theta^*) + (\Xi - \Xi^*) \Big\| \leq \frac{1}{\delta} \|\varepsilon\| \Big(\|\Theta - \Theta^*\| + \|\Xi - \Xi^*\| \Big). \tag{3.9}$$

When $\boldsymbol{y} - \boldsymbol{y}^* \in \text{Eigvecs}(\boldsymbol{A} + \boldsymbol{E}_m)$ $\Big(\boldsymbol{y} - \boldsymbol{y}^* \in \text{Eigvecs}(\boldsymbol{A} - \boldsymbol{E}_m)\Big)$, we have $\big\|(\boldsymbol{A} + \boldsymbol{E}_m)(\boldsymbol{y} - \boldsymbol{y}^*)\big\| \leq \rho(\boldsymbol{A} + \boldsymbol{E}_m)\|\boldsymbol{y} - \boldsymbol{y}^*\|$ $\Big(\big\|(\boldsymbol{A} - \boldsymbol{E}_m)(\boldsymbol{y} - \boldsymbol{y}^*)\big\| \leq \rho(\boldsymbol{A} - \boldsymbol{E}_m)\|\boldsymbol{y} - \boldsymbol{y}^*\|\Big)$ by utilizing the homogeneity of the matrix norm and [28, Theorem 5.6.9.]. Otherwise, by the compatibility (see [29, Remark 1]) of the matrix spectral norm and the vector ℓ_2-norm, we have

$$\big\|(\boldsymbol{A} + \boldsymbol{E}_m)(\boldsymbol{y} - \boldsymbol{y}^*)\big\| \leq \|\boldsymbol{A} + \boldsymbol{E}_m\|_2 \|\boldsymbol{y} - \boldsymbol{y}^*\|$$

and

$$\big\|(\boldsymbol{A} - \boldsymbol{E}_m)(\boldsymbol{y} - \boldsymbol{y}^*)\big\| \leq \|\boldsymbol{A} - \boldsymbol{E}_m\|_2 \|\boldsymbol{y} - \boldsymbol{y}^*\|.$$

Utilizing (3.9), Lemma 3.1, and the definitions of $\Theta(\cdot)$ and $\Xi(\cdot)$, one deduces

$$\|\boldsymbol{y} - \boldsymbol{y}^*\|^2 \leq \frac{1}{\delta} \|\varepsilon\| \Big[\|(\boldsymbol{A} + \boldsymbol{E}_m)(\boldsymbol{y} - \boldsymbol{y}^*)\| + \|(\boldsymbol{A} - \boldsymbol{E}_m)(\boldsymbol{y} - \boldsymbol{y}^*)\| \Big] \leq \frac{\kappa_1 + \kappa_2}{\delta} \|\varepsilon\| \|\boldsymbol{y} - \boldsymbol{y}^*\|,$$

namely,

$$\|\boldsymbol{y} - \boldsymbol{y}^*\| \leq \frac{\kappa_1 + \kappa_2}{\delta} \|\varepsilon\| = \frac{\kappa_1 + \kappa_2}{\delta} \|\Lambda(\boldsymbol{y})\|, \tag{3.10}$$

where κ_1 and κ_2 are defined by (3.2) and (3.3), respectively. From the definitions of κ_1, κ_2 and the spectral norm, it follows that $\kappa_1 \geq 0$ and $\kappa_2 \geq 0$ are always true and $\kappa_1 = 0$ ($\kappa_2 = 0$) iff $\boldsymbol{A} = -\boldsymbol{E}_m$ ($\boldsymbol{A} = \boldsymbol{E}_m$), so $\kappa_1 + \kappa_2 > 0$ must be established. From (3.10), it then follows that the right-hand inequality of (3.1) holds.

Besides, for any $\boldsymbol{y} \in \mathbb{R}^m$ and $\boldsymbol{z} \in \mathbb{R}^m$, if $\boldsymbol{y} - \boldsymbol{z} \in \text{Eigvecs}(\boldsymbol{A} + \boldsymbol{E}_m)$, then $\big\|(\boldsymbol{A} + \boldsymbol{E}_m)(\boldsymbol{y} - \boldsymbol{z})\big\| \leq \rho(\boldsymbol{A} + \boldsymbol{E}_m)\|\boldsymbol{y} - \boldsymbol{z}\|$ by using [28, Theorem 5.6.9.] and the homogeneity of the matrix norm;

otherwise, it follows from [29, Remark 1] that we obtain $\|(A+E_m)(y-z)\| \leq \|A+E_m\|_2\|y-z\|$. So, by the definitions of $\Theta(\cdot)$ and κ_1, we conclude that

$$\|\Theta(y)-\Theta(z)\| = \|(A+E_m)(y-z)\| \leq \kappa_1\|y-z\|, \ \forall y,z \in \mathbb{R}^m. \tag{3.11}$$

It then follows from (3.11) that $\Theta(\cdot)$ is globally Lipschitz continuous with the Lipschitz constant $\mathscr{L}=\kappa_1$. By (3.4) and (3.5), one has

$$\|\varepsilon\|^2 \leq \langle \Theta-\Theta^*, \Xi-\Xi^* \rangle + \|\varepsilon\|^2 \leq \langle \varepsilon, (\Theta-\Theta^*)+(\Xi-\Xi^*) \rangle. \tag{3.12}$$

Utilizing the Cauchy-Schwarz inequality, the triangle inequality, Lemma 3.1, [28, Theorem 5.6.9.], [29, Remark 1], and the definitions of $\Theta(\cdot)$ and $\Xi(\cdot)$, we see from (3.2), (3.3), and (3.12) that

$$\|\varepsilon\|^2 \leq \|\varepsilon\|\Big(\|\Theta-\Theta^*\|+\|\Xi-\Xi^*\|\Big) \leq (\kappa_1+\kappa_2)\|\varepsilon\|\|y-y^*\|,$$

that is,

$$\frac{1}{\kappa_1+\kappa_2}\|\Lambda(y)\| = \frac{1}{\kappa_1+\kappa_2}\|\varepsilon\| \leq \|y-y^*\|. \tag{3.13}$$

It thus follows from (3.13) that the left-hand inequality of (3.1) is true. Hence, the conclusion is established. □

Remark 3.1. It is worth noticing that one deduces that $\kappa_1+\kappa_2$ in (3.1) is less than or equal to L_1+L_2 involved in [23, Theorem 4.1] by utilizing the property (see [28, Theorem 5.6.9.]) of spectral radius and the compatibility (see [29, Remark 1]) of the matrix spectral norm and the vector ℓ_2-norm. Hence, theoretically, the upper and lower bounds of the error involved in this paper are more compact than those in [23], which shows that we have improved the results in [23].

For notational simplicity, (t) will be omitted for all variables $\big($like $y(t)\big)$ containing (t) in the remainder of this work, unless necessary. Now, we propose the following inverse-free dynamical system (IFDS),

$$\dot{y} = -h\Big[\alpha\|\Lambda(y)\|_p^{\mu}+\beta\|\Lambda(y)\|_q^{\nu}\Big]\mathscr{H}(y), \tag{3.14}$$

where $\mathscr{H}(y)=A^\top\Lambda(y)$, $\Lambda(y)=Ay-|y|-b$, and h, α, β, p, $q \in \mathbb{R}_+$ and μ, $\nu \in \mathbb{R}$ are the designed parameters.

Remark 3.2. The proposed IFDS (3.14) is inspired from the inverse-free dynamical system in [23]. From the concise structure of (3.14), it can be seen that IFDS inherits the advantages of the dynamical system in [23], that is, it can directly solve AVE (1.1) and does not involve any matrix inversion operation. Furthermore, it is worth noting that when $\mu=\nu=0$, IFDS (3.14) degenerates to the dynamical system in [23]. And we deduce that the reduced dynamical system is globally exponentially stable (see Theorem 4.4 for details).

Now, we give a lemma on the relationship between the equilibrium point (defined by Definition 2.1) of IFDS (3.14) and the solution to AVE (1.1).

Lemma 3.2. *Under Assumption 2.1, if $y^* \in \mathbb{R}^m$ is an equilibrium point of IFDS (3.14) iff it is the solution to AVE (1.1).*

Proof. From Definition 2.1, it follows that if $\boldsymbol{y}^* \in \mathbb{R}^m$ is an equilibrium point to IFDS (3.14), then

$$\left[\alpha\left\|\Lambda(\boldsymbol{y}^*)\right\|_p^{\mu} + \beta\left\|\Lambda(\boldsymbol{y}^*)\right\|_q^{\nu}\right]\mathscr{H}(\boldsymbol{y}^*) = \boldsymbol{0},$$

namely,

$$\alpha\left\|\Lambda(\boldsymbol{y}^*)\right\|_p^{\mu} + \beta\left\|\Lambda(\boldsymbol{y}^*)\right\|_q^{\nu} = 0, \tag{3.15}$$

or

$$\mathscr{H}(\boldsymbol{y}^*) = \boldsymbol{0}. \tag{3.16}$$

To implement the IFDS (3.14) well, we set $\left\|\Lambda(\boldsymbol{y})\right\|_p^{\mu} \triangleq 0$ ($\left\|\Lambda(\boldsymbol{y})\right\|_q^{\nu} \triangleq 0$) when $\mu = 0$ ($\nu = 0$) and $\Lambda(\boldsymbol{y}) = \boldsymbol{0}$, and $\left\|\Lambda(\boldsymbol{y})\right\|_p^{\mu}\mathscr{H}(\boldsymbol{y}) \triangleq 0$ ($\left\|\Lambda(\boldsymbol{y})\right\|_q^{\nu}\mathscr{H}(\boldsymbol{y}) \triangleq 0$) when $\mu < 0$ ($\nu < 0$) and $\Lambda(\boldsymbol{y}) = \boldsymbol{0}$. That is to say that we let $0^0 = 0$ and $\frac{0}{0} = 0$ in this paper. Consequently, by (3.14) and (3.15), one has

$$\Lambda(\boldsymbol{y}^*) = \boldsymbol{A}\boldsymbol{y}^* - \left|\boldsymbol{y}^*\right| - \boldsymbol{b} = \boldsymbol{0}. \tag{3.17}$$

Note that from Assumption 2.1 it can be directly obtained that $\boldsymbol{A} \in \mathbb{R}^{m\times m}$ is invertible. It thus follows from (3.14) and (3.16) that

$$\boldsymbol{A}^{\top}\Lambda(\boldsymbol{y}^*) = \boldsymbol{0} \;\Leftrightarrow\; \Lambda(\boldsymbol{y}^*) = \boldsymbol{0}. \tag{3.18}$$

By (3.17) and (3.18), one has $\boldsymbol{A}\boldsymbol{y}^* - \left|\boldsymbol{y}^*\right| - \boldsymbol{b} = \boldsymbol{0}$. It then follows from Lemma 2.1 that $\boldsymbol{y}^*$ is the solution to AVE (1.1). Besides, if a point $\boldsymbol{y}^*$ is a solution to AVE (1.1), it is not difficult to find that it is the equilibrium point of IFDS (3.14). That is, the converse is also true. This proof is finished. □

4. Main Results

In this section, we begin to prove that IFDS (3.14) is globally asymptotic, sublinear and exponential convergent under Assumption 2.1 and various parameters, respectively. At first, Lipschitz continuity of the function $\mathscr{H}(\boldsymbol{y})$ in (3.14) is presented as follows.

Lemma 4.1. *The mapping $\mathscr{H}(\cdot) : \mathbb{R}^m \to \mathbb{R}^m$ involved in IFDS (3.14) is globally Lipschitz continuous.*

Proof. Combining (3.14) and the compatibility [29] of the spectral norm, one deduces

$$\begin{aligned}\left\|\mathscr{H}(\boldsymbol{y}) - \mathscr{H}(\boldsymbol{z})\right\| &= \left\|\boldsymbol{A}^{\top}\boldsymbol{A}(\boldsymbol{y}-\boldsymbol{z}) + \boldsymbol{A}^{\top}(|\boldsymbol{z}| - |\boldsymbol{y}|)\right\| \\ &\le \left\|\boldsymbol{A}^{\top}\boldsymbol{A}(\boldsymbol{y}-\boldsymbol{z})\right\| + \left\|\boldsymbol{A}^{\top}(|\boldsymbol{y}| - |\boldsymbol{z}|)\right\|\end{aligned} \tag{4.1}$$

for any $\boldsymbol{y} \in \mathbb{R}^m$ and $\boldsymbol{z} \in \mathbb{R}^m$. By the proof of Lemma 3.1, it can be obtained that

$$\left\|\boldsymbol{A}^{\top}\boldsymbol{A}(\boldsymbol{y}-\boldsymbol{z})\right\| \le \mathscr{L}_1\left\|\boldsymbol{y}-\boldsymbol{z}\right\| \tag{4.2}$$

and

$$\left\|\boldsymbol{A}^{\top}(|\boldsymbol{y}| - |\boldsymbol{z}|)\right\| \le \mathscr{L}_2\left\||\boldsymbol{y}| - |\boldsymbol{z}|\right\|, \tag{4.3}$$

where

$$\eta_1 \triangleq \begin{cases} \rho(\boldsymbol{A}^{\top}\boldsymbol{A}), & \boldsymbol{x}-\boldsymbol{y} \in \mathrm{Eigvecs}(\boldsymbol{A}^{\top}\boldsymbol{A}), \\ \left\|\boldsymbol{A}^{\top}\boldsymbol{A}\right\|_2, & \text{otherwise}, \end{cases}$$

with $\rho\left(\boldsymbol{A}^{\top}\boldsymbol{A}\right) \triangleq \max\left\{\left|\lambda\right| : \lambda \in \text{Eigvals}\left(\boldsymbol{A}^{\top}\boldsymbol{A}\right)\right\}$ denoting the spectral radius of $\boldsymbol{A}^{\top}\boldsymbol{A}$, and

$$\eta_2 \triangleq \begin{cases} \rho\left(\boldsymbol{A}^{\top}\right), & |\boldsymbol{x}| - |\boldsymbol{y}| \in \text{Eigvecs}\left(\boldsymbol{A}^{\top}\right), \\ \|\boldsymbol{A}\|_2, & \text{otherwise}, \end{cases}$$

with $\rho\left(\boldsymbol{A}^{\top}\right) \triangleq \max\left\{\left|\lambda\right| : \lambda \in \text{Eigvals}\left(\boldsymbol{A}^{\top}\right)\right\}$ being the spectral radius of $\boldsymbol{A}^{\top}$. It thus follows from (4.1), (4.2), and (4.3) that

$$\left\|\mathscr{H}(\boldsymbol{y}) - \mathscr{H}(\boldsymbol{z})\right\| \leq \eta_1\left\|\boldsymbol{y}-\boldsymbol{z}\right\| + \eta_2\left\||\boldsymbol{y}| - |\boldsymbol{z}|\right\|. \tag{4.4}$$

By (4.4) and the fact that $\left\||\boldsymbol{y}| - |\boldsymbol{z}|\right\| \leq \left\|\boldsymbol{y}-\boldsymbol{z}\right\|$, one sees that

$$\left\|\mathscr{H}(\boldsymbol{y}) - \mathscr{H}(\boldsymbol{z})\right\| \leq \left(\eta_1 + \eta_2\right)\left\|\boldsymbol{y}-\boldsymbol{z}\right\|. \tag{4.5}$$

It then follows from (4.5) that $\mathscr{H}(\cdot) : \mathbb{R}^m \to \mathbb{R}^m$ is globally Lipschitz continuous with the Lipschitz constant $\eta_0 = \eta_1 + \eta_2$. This completes the proof. □

Remark 4.1. It is worth mentioning that our modulus η_0 is tighter than that in [23] since $\left\|\boldsymbol{A}^{\top}\right\|_2\left\|\boldsymbol{A}\right\|_2 \geq \eta_1$ and $\left\|\boldsymbol{A}^{\top}\right\|_2 \geq \eta_2$. Besides, it can be obtained from [15, Lemma 3] that $\mathscr{H}(\cdot)$ is a Lipschitz continuous vector field. Thus, IFDS (3.14) possesses a unique equilibrium point by virtue of [15, Lemma 3] and Lemma 4.1.

Let $\mu \neq 0$ or $\nu \neq 0$ in (3.14). In what follows, the stability and global convergence results of IFDS (3.14) is established.

Theorem 4.1. *Suppose that Assumption 2.1 is satisfied. If $\mu \neq 0$ or $\nu \neq 0$, then, for any initial point $\boldsymbol{y}(t_0) \in \mathbb{R}^m$, IFDS (3.14) is stable in the Lyapunov sense, and its solution trajectory $\boldsymbol{y}(t)$ converges globally to the solution to AVE (1.1).*

Proof. Let us consider the Lyapunov function candidate:

$$H\left(\boldsymbol{y}(t)\right) \triangleq \left\|\boldsymbol{y}(t) - \boldsymbol{y}^*\right\|^2. \tag{4.6}$$

For the sake of simplification discussed, (t) will be omitted for the variable $\boldsymbol{y}(t)$ in the remainder of this work, unless necessary. By (4.6), one has

$$H(\boldsymbol{y}) \geq \frac{1}{2}\left\|\boldsymbol{y}-\boldsymbol{y}^*\right\|^2, \tag{4.7}$$

which implies that $H(\boldsymbol{y}) = 0$ iff $\boldsymbol{y} = \boldsymbol{y}^*$, and $H(\boldsymbol{y}) \to +\infty$ when $\|\boldsymbol{y}\| \to +\infty$. On the one hand, $H(\boldsymbol{y}) \geq 0$ needs to be verified. From (4.6), it is not difficult to obtain that $H\left(\boldsymbol{y}^*\right) = 0$ for $\boldsymbol{y} = \boldsymbol{y}^*$ and $H(\boldsymbol{y}) > 0$ for any $\boldsymbol{y} \neq \boldsymbol{y}^*$.

On the other hand, the differentiation of $H(\cdot)$ with respect to t, namely, $\dot{H}(\boldsymbol{y}) = \frac{dH(\boldsymbol{y})}{d\boldsymbol{y}} \cdot \frac{d\boldsymbol{y}}{dt} \leq 0$ needs to be demonstrated. From (3.14) and the definition of $H(\cdot)$ in (4.6), it follows that

$$\begin{aligned} \dot{H}(\boldsymbol{y}) =& -2h\Big\langle \boldsymbol{y}-\boldsymbol{y}^*, \left[\alpha\left\|\Lambda(\boldsymbol{y})\right\|_p^{\mu} + \beta\left\|\Lambda(\boldsymbol{y})\right\|_q^{\nu}\right]\boldsymbol{A}^{\top}\Lambda(\boldsymbol{y})\Big\rangle \\ =& -2h\alpha\left\|\Lambda(\boldsymbol{y})\right\|_p^{\mu}\left\langle \boldsymbol{y}-\boldsymbol{y}^*, \boldsymbol{A}^{\top}\Lambda(\boldsymbol{y})\right\rangle - 2h\beta\left\|\Lambda(\boldsymbol{y})\right\|_q^{\nu}\left\langle \boldsymbol{y}-\boldsymbol{y}^*, \boldsymbol{A}^{\top}\Lambda(\boldsymbol{y})\right\rangle. \end{aligned} \tag{4.8}$$

It then follows from (3.14), (4.8), and Lemma 2.2 that

$$\dot{H}(\boldsymbol{y}) \leq -h\left\|\Lambda(\boldsymbol{y})\right\|^2\left[\alpha\left\|\Lambda(\boldsymbol{y})\right\|_p^{\mu} + \beta\left\|\Lambda(\boldsymbol{y})\right\|_q^{\nu}\right] \leq 0, \tag{4.9}$$

which indicates that $H(\cdot)$ is non-increasing. Moreover, if $\dot{H}(\boldsymbol{y}) = 0$, then it follows from (4.9) and Lemma 3.2 that $\Lambda(\boldsymbol{y}) = \boldsymbol{0}$ holds, that is, $\dot{\boldsymbol{y}} = \boldsymbol{0}$ is established. Thus, one draws the conclusion: $H(\boldsymbol{y})$ is a Lyapunov function.

For all $t \geq t_0$ and fixed $t_0 \in \mathbb{R}_+ \cup \{0\}$, $H\big(\boldsymbol{y}(t)\big) \leq H\big(\boldsymbol{y}(t_0)\big)$ since $H(\cdot)$ is non-increasing. By (4.7), one has

$$\frac{1}{2}\left\|\boldsymbol{y}(t) - \boldsymbol{y}^*\right\|^2 \leq H\big(\boldsymbol{y}(t)\big) \leq H\big(\boldsymbol{y}(t_0)\big),\ t \in [t_0, +\infty). \tag{4.10}$$

It then follows from (4.9) and (4.10) that $H\big(\boldsymbol{y}(t)\big)$ has a finite limit as $t \to +\infty$, and each trajectory $\boldsymbol{y}(t)$ is uniformly bounded on $[t_0, +\infty)$. By the boundedness of the trajectory $\boldsymbol{y}(t)$, it can be deduced that there exists a monotonically increasing sequence $\{t_j\}_{j=1}^{+\infty}$ and a point $\tilde{\boldsymbol{y}}$ such that $\lim_{j \to +\infty} \boldsymbol{y}(t_j) = \tilde{\boldsymbol{y}}$. Consequently, $\tilde{\boldsymbol{y}}$ is limit point of $\boldsymbol{y}(t)$. In light of the LaSalle invariance principle in [26], $\boldsymbol{y}$ converges to the largest invariant subset of the set $S = \{\boldsymbol{y} \in \mathbb{R}^m : \dot{H}(\boldsymbol{y}) = 0\}$ when $t \to +\infty$. It is noticed that $\boldsymbol{y} = \boldsymbol{y}^*$ when $\dot{H}(\boldsymbol{y}) = 0$. Then, the trajectory $\boldsymbol{y}(t)$ converges to the equilibria set as $t \to +\infty$. Accordingly, the limit point $\tilde{\boldsymbol{y}}$ is an equilibria.

Now we conclude that $\lim_{t \to +\infty} \boldsymbol{y}(t) = \tilde{\boldsymbol{y}}$ holds for each initial point $\boldsymbol{y}(t_0)$. Replacing $\boldsymbol{y}^*$ with $\tilde{\boldsymbol{y}}$ in (4.6), we design a new Lyapunov function

$$\hat{H}(\boldsymbol{y}) = \left\|\boldsymbol{y} - \tilde{\boldsymbol{y}}\right\|^2. \tag{4.11}$$

Similar to the calculation of $\dot{H}(\boldsymbol{y})$, it follows from (4.11) that $\dot{\hat{H}}(\boldsymbol{y}) \leq 0$ holds for all $t \in [t_0, +\infty)$. Due to $\hat{H}(\boldsymbol{y}) \geq 0$ and the continuity of the function $\hat{H}(\cdot)$, for any sufficiently small positive number $\tilde{\varepsilon}$, there exists a positive natural number k and a positive constant $\tilde{\delta}$ such that $\big|\hat{H}\big(\boldsymbol{y}(t_k)\big) - \hat{H}(\tilde{\boldsymbol{y}})\big| = \big|\hat{H}\big(\boldsymbol{y}(t_k)\big)\big| = \hat{H}\big(\boldsymbol{y}(t_k)\big) < \tilde{\varepsilon}$ when $\left\|\boldsymbol{y}(t_k) - \tilde{\boldsymbol{y}}\right\| < \tilde{\delta}$, where $t_k \in (t_0, +\infty)$. Furthermore, based on the monotone nonincreasing property of $\hat{H}(\cdot)$, $\hat{H}\big(\boldsymbol{y}(t)\big) \leq \hat{H}\big(\boldsymbol{y}(t_k)\big) < \tilde{\varepsilon}$ holds for arbitrary $t \in [t_k, +\infty)$. This shows that $\lim_{t \to +\infty} \boldsymbol{y}(t) = \tilde{\boldsymbol{y}}$ holds. Then, by $\lim_{\|\boldsymbol{y}\| \to +\infty} \hat{H}(\boldsymbol{y}) = +\infty$, we conclude that the solution trajectories $\boldsymbol{y}(t) \in \mathbb{R}^m$ of IFDS (3.14) converges globally to the solution of AVE (1.1). If there is a unique solution to AVE (1.1), then the solution trajectory $\boldsymbol{y}(t) \in \mathbb{R}^m$ is asymptotically stable for any initial vector $\boldsymbol{y}(t_0) \in \mathbb{R}^m$. This proof is completed. □

Next, under various parameter conditions, the global sublinear convergence of IFDS (3.14) is obtained by utilizing the new global error bound formula (see Lemma 3.1).

Theorem 4.2. *Suppose that Assumption 2.1 holds. For any initial point $\boldsymbol{y}(t_0) \in \mathbb{R}^m$, the tracking error $\left\|\boldsymbol{y}(t) - \boldsymbol{y}^*\right\|$ associated with IFDS (3.14) achieves a nonergodic sublinear convergence rate $\mathscr{O}\big((\frac{1}{t})^{\zeta_1}\big)$ if anyone of the following two statements is satisfied:*

(i) $\zeta_1 \triangleq \frac{1}{\nu}$, $\mu \neq 0$, $\nu > 0$ *and* $q \in (0, 2]$.

(ii) $\zeta_1 \triangleq \frac{1}{\mu}$, $\mu > 0$, $\nu \neq 0$ *and* $p \in (0, 2]$.

Proof. (i) Now we consider the Lyapunov function $H(\boldsymbol{y}) \triangleq \left\|\boldsymbol{y} - \boldsymbol{y}^*\right\|^2$ defined in (4.6). By the definition of $H(\cdot)$ and the proof of Theorem 4.1, one has

$$\dot{H} \leq -h\alpha\left\|\Lambda(\boldsymbol{y})\right\|^2\left\|\Lambda(\boldsymbol{y})\right\|_p^{\mu} - h\beta\left\|\Lambda(\boldsymbol{y})\right\|^2\left\|\Lambda(\boldsymbol{y})\right\|_q^{\nu}. \tag{4.12}$$

Based on $\|\Lambda(\boldsymbol{y})\|_q \geq \|\Lambda(\boldsymbol{y})\|$ for any $q \in (0,2]$ (see the inequality (7) in [30]) and $\nu > 0$, (4.12) implies that

$$\dot{H} \leq -h\beta \|\Lambda(\boldsymbol{y})\|^{\nu+2}. \tag{4.13}$$

Furthermore, by (3.1) in Lemma 3.1, it is straightforward to conclude

$$\|\Lambda(\boldsymbol{y})\| \geq \frac{\delta}{\kappa_1+\kappa_2}\|\boldsymbol{y}-\boldsymbol{y}^*\|. \tag{4.14}$$

It then follows from (4.13) and (4.14) that

$$\dot{H} \leq -c\|\boldsymbol{y}-\boldsymbol{y}^*\|^{\nu+2}, \tag{4.15}$$

where $c = h\beta\left(\frac{\delta}{\kappa_1+\kappa_2}\right)^{\nu+2}$. By (4.6) and (4.15), one deduces

$$\|\boldsymbol{y}-\boldsymbol{y}^*\| \leq \|\boldsymbol{y}(t_0)-\boldsymbol{y}^*\|\left(\frac{2}{c\nu}\cdot\frac{1}{t}\right)^{\frac{1}{\nu}},$$

namely, $\|\boldsymbol{y}-\boldsymbol{y}^*\| = \mathscr{O}\left(\left(\frac{1}{t}\right)^{\zeta_1}\right)$ with $\zeta_1 = \frac{1}{\nu}$, which indicates that the tracking error $\|\boldsymbol{y}(t)-\boldsymbol{y}^*\|$ associated with IFDS (3.14) achieves $\mathscr{O}\left(\left(\frac{1}{t}\right)^{\zeta_1}\right)$. Consequently, (i) holds.

(ii) The proof of part (ii) is completely similar to parts (i), thus we omit it here. This completes the proof. □

Theorem 4.3. *Under Assumption 2.1, for each initial value $\boldsymbol{y}(t_0) \in \mathbb{R}^m$ in IFDS (3.14), the tracking error $\|\boldsymbol{y}(t)-\boldsymbol{y}^*\|$ satisfies*

$$\|\boldsymbol{y}(t)-\boldsymbol{y}^*\| \leq \left\|\boldsymbol{y}(t_0)-\boldsymbol{y}^*\right\|\left(\gamma\cdot\frac{1}{t}\right)^{\zeta_2},$$

that is to say that the error associated with IFDS (3.14) achieves a nonergodic sublinear convergence rate $\mathscr{O}\left(\left(\frac{1}{t}\right)^{\zeta_2}\right)$, if anyone of the following two statements is true:

(i) $\zeta_2 \triangleq \frac{1}{\mu}$, $\mu > 0$, $\nu < 0$, $0 < p \leq 2$, $q \geq 2$ *and* $\gamma = \frac{2(\kappa_1+\kappa_2)^{\nu+2}}{h\alpha\mu\delta^{\nu+2}}$;

(ii) $\zeta_2 \triangleq \frac{1}{\nu}$, $\mu < 0$, $\nu > 0$, $p \geq 2$, $0 < q \leq 2$ *and* $\gamma = \frac{2(\kappa_1+\kappa_2)^{\mu+2}}{h\beta\nu\delta^{\mu+2}}$.

Proof. This proof is similar to Theorem 4.2, and thus is omitted. □

Remark 4.2. From Theorems 4.2 and 4.3, under different parameter settings, it can be seen that the global tracking error associated with IFDS (3.14) achieves zero with the nonergodic sublinear convergence rate, and we can flexibly adjust the sublinear convergence rate. Furthermore, for addressing AVE (1.1), the selection of these different parameters is not complicated, which is quite convenient for the implementation of our system.

It is worth noting that IFDS (3.14) with $\mu = \nu = 0$ is the dynamical system (3.8) in [23]. In what follows, we investigate the global exponential convergence for the proposed dynamical system in this case.

Theorem 4.4. *If Assumption 2.1 and $\mu = \nu = 0$ hold, then, for any initial vector $\boldsymbol{y}(t_0) \in \mathbb{R}^m$, IFDS (3.14) is exponentially convergent.*

Proof. We consider the Lyapunov function $H\big(\boldsymbol{y}(t)\big)$ defined in (4.6). By (4.6), one has

$$\frac{1}{2}\left\|\boldsymbol{y}(t)-\boldsymbol{y}^*\right\|^2 \leq H\big(\boldsymbol{y}(t)\big) \leq \frac{3}{2}\left\|\boldsymbol{y}(t)-\boldsymbol{y}^*\right\|^2,$$

namely,

$$\frac{2}{3}H\big(\boldsymbol{y}(t)\big) \leq \left\|\boldsymbol{y}(t)-\boldsymbol{y}^*\right\|^2 \leq 2H\big(\boldsymbol{y}(t)\big). \tag{4.16}$$

It follows from (3.14) and $\mu=\nu=0$ that

$$\dot{\boldsymbol{y}}(t) = -h\boldsymbol{A}^\top\Lambda\big(\boldsymbol{y}(t)\big). \tag{4.17}$$

Moreover, by (3.1) in Lemma 3.1, we obtain that

$$\frac{\delta}{\kappa_1+\kappa_2}\left\|\boldsymbol{y}(t)-\boldsymbol{y}^*\right\| \leq \Lambda\big(\boldsymbol{y}(t)\big) \leq \big(\kappa_1+\kappa_2\big)\left\|\boldsymbol{y}(t)-\boldsymbol{y}^*\right\|. \tag{4.18}$$

It then follows from (4.6), (4.16)-(4.18) and Lemma 2.2 that

$$\begin{aligned}\frac{dH\big(\boldsymbol{y}(t)\big)}{dt} &= 2\big\langle\dot{\boldsymbol{y}}(t),\boldsymbol{y}(t)-\boldsymbol{y}^*\big\rangle = -2h\Big\langle\boldsymbol{A}^\top\Lambda\big(\boldsymbol{y}(t)\big),\boldsymbol{y}(t)-\boldsymbol{y}^*\Big\rangle\\ &\leq -h\Big\|\Lambda\big(\boldsymbol{y}(t)\big)\Big\|^2 \leq -\frac{h\delta^2}{\big(\kappa_1+\kappa_2\big)^2}\left\|\boldsymbol{y}(t)-\boldsymbol{y}^*\right\|^2 \leq -\frac{2h\delta^2}{3\big(\kappa_1+\kappa_2\big)^2}H\big(\boldsymbol{y}(t)\big).\end{aligned} \tag{4.19}$$

Set $c \triangleq \dfrac{2h\delta^2}{3\big(\kappa_1+\kappa_2\big)^2} \in \mathbb{R}_+$. Then, (4.19) is rewritten as:

$$\frac{dH\big(\boldsymbol{y}(t)\big)}{dt} \leq -cH\big(\boldsymbol{y}(t)\big). \tag{4.20}$$

Thus, for each $t \geq t_0$, integrating (4.20) from t_0 to t implies

$$H\big(\boldsymbol{y}(t)\big) \leq H\big(\boldsymbol{y}(t_0)\big)\exp\big(-c\big(t-t_0\big)\big). \tag{4.21}$$

In addition, by utilizing (4.6) and (4.21), one has

$$\left\|\boldsymbol{y}(t)-\boldsymbol{y}^*\right\| \leq \sqrt{H\big(\boldsymbol{y}(t_0)\big)}\exp\big(-\tau\big(t-t_0\big)\big), \qquad \forall\, t \geq t_0, \tag{4.22}$$

where $\tau \triangleq \frac{c}{2}$. By (4.22) and Definition 2.2, one obtains that IFDS (3.14) is exponentially convergent for any initial value $\boldsymbol{y}(t_0) \in \mathbb{R}^m$. This proof is completed. □

5. Experimental results

This section provides a numerical example to illustrate the computation performance and theoretical results of our dynamical system. The ODE45 solver in MATLAB R2019b is used to implement the numerical simulations on the dynamical system (3.8) in [23] and IFDS (3.14) in this work. For all comparison dynamical systems, we choose the same initial points. For the dynamical system (3.8) in [23], we take $\gamma = 100$; for IFDS (3.14), we take $h = 100$ and $\alpha = \beta = 1$. To evaluate the performance of those systems, the tracking error of AVE (1.1) is described by $\mathscr{E} = \left\|\boldsymbol{y}-\boldsymbol{y}^*\right\|$, where $\boldsymbol{y}^*$ stands for the solution to AVE (1.1).

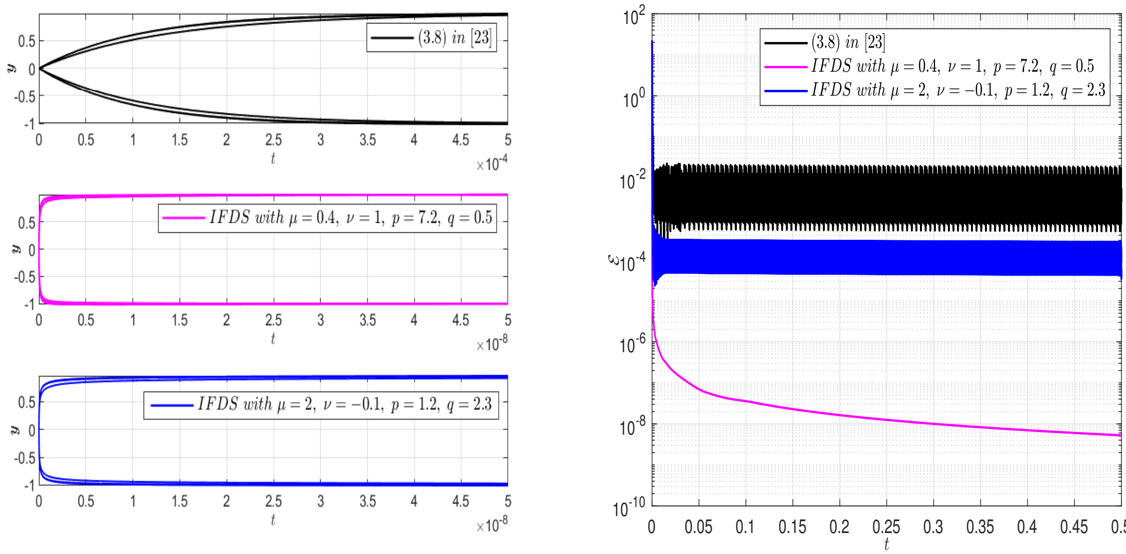

(a) (b)

FIGURE 1. For (3.8) in [23] and IFDS: (a) Convergence behaviors. (b) Computation errors.

Example 1 [31]: Consider a class of AVE (1.1) with $\boldsymbol{A} = \text{tridiag}\big(-1,8,-1\big) \in \mathbb{R}^m$ and $\boldsymbol{b} = \boldsymbol{A}\boldsymbol{y}^* - \big|\boldsymbol{y}^*\big| \in \mathbb{R}^m$, where

$$\begin{cases} \text{tridiag}(-1,8,-1) = \begin{bmatrix} 8 & -1 & & & & \\ -1 & 8 & -1 & & & \\ & -1 & 8 & & & \\ & & & \ddots & -1 & \\ & & & -1 & 8 & -1 \\ & & & & -1 & 8 \end{bmatrix}, \\ \boldsymbol{y}^* = \big(-1,1,-1,1,\cdots,-1,1\big)^\top. \end{cases}$$

From Example 1, it can be obtained that $\lambda_{\min}(\boldsymbol{A}^\top\boldsymbol{A}) > 1$, which indicates that Assumption 2.1 holds. For IFDS (3.14), we choose $\mu = 0.4$, $\nu = 1$, $p = 7.2$, $q = 0.5$, and $\mu = 2$, $\nu = -0.1$, $p = 1.2$, and $q = 2.3$, respectively. We take the same initial vector $\boldsymbol{y}_0 = zeros(m,1)$ in all comparison dynamical systems. For Example 1 with $m = 500$, the convergence behaviors and tracking errors of these comparison dynamical systems are reported in Fig. 1(a)-(b). It can be observed from Fig. 1(a)-(b) that all systems quickly stabilize to the solution of Example 1. However, compared with the dynamical system (3.8) in [23], our system converges to the solution of the absolute value equations faster, and the amplitude of the tracking error corresponding to our system is smaller. Furthermore, it can be seen from Fig. 1(a) that our systems enjoy higher computation accuracy than the dynamical system (3.8) in [23]. For Example 1 with $m = 100$, Fig. 2(a)-(b) reports the tracking error convergence results of IFDS with $\mu \neq 0$, $\nu > 0$, $p > 0$, $0 < q \leq 2$ and IFDS with $\mu > 0$, $\nu < 0$, $0 < p \leq 2$, $q \geq 2$ for different values of μ, ν, p and q. From Fig. 2(a), it can be seen that when $\mu = 0.4$, $\nu = 1$, $p = 7.2$ and $q = 0.5$, the corresponding system has the

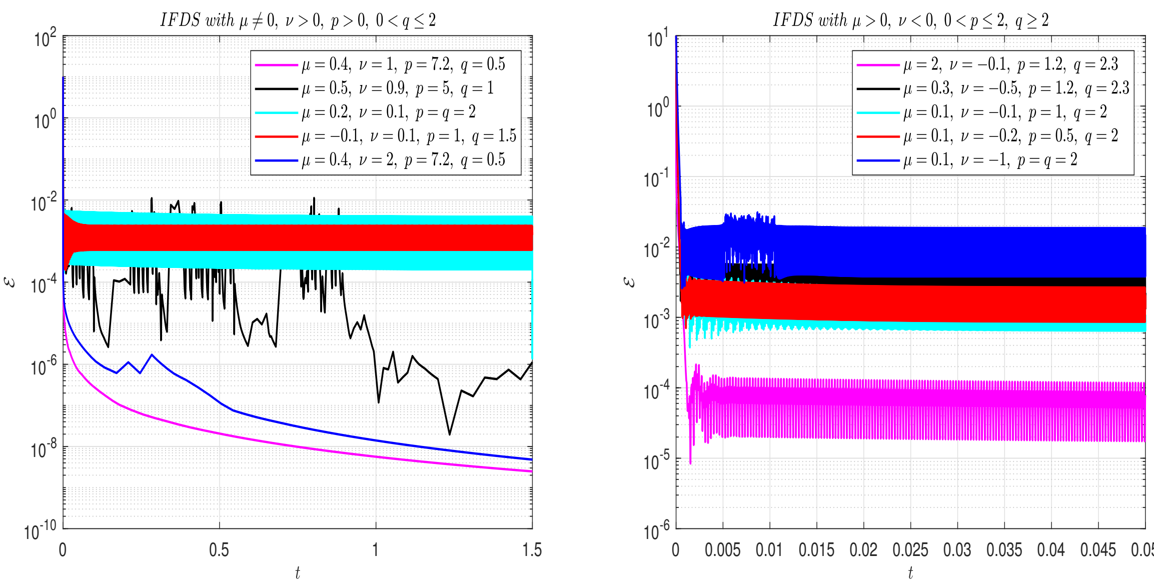

(a) (b)

FIGURE 2. (a) Effect of the parameters for IFDS with $\mu \neq 0$, $\nu > 0$, $p > 0$ and $0 < q \leq 2$. (b) Effect of the parameters for IFDS with $\mu > 0$, $\nu < 0$, $0 < p \leq 2$ and $q \geq 2$.

TABLE 1. Comparison results of three different dynamical systems for Example 1

Example 1 ([31]) setting		(3.8) in [23]	IFDS with $\mu = 0.4$, $\nu = 1$, $p = 7.2$, $q = 0.5$	IFDS with $\mu = 2$, $\nu = -0.1$, $p = 1.2$, $q = 2.3$
$\boldsymbol{y}_0$	m	$\mathscr{E}$	$\mathscr{E}$	$\mathscr{E}$
	1000	$3.9769e-03$	**2.5707e-09**	**1.0524e-05**
	2000	$5.6837e-02$	**9.6075e-10**	**8.7570e-06**
$zeros(m,1)$	3000	$7.2237e-03$	**2.2317e-10**	**1.5731e-06**
	5000	$9.4100e-03$	**2.4176e-04**	**1.0310e-06**

highest error accuracy. This is why we choose $\mu = 0.4$, $\nu = 1$, $p = 7.2$ and $q = 0.5$ as the design parameters of IFDS with $\mu \neq 0$, $\nu > 0$, $p > 0$, $0 < q \leq 2$ in Fig. 1(a). For the same reason, the most appropriate choice of the design parameters of IFDS with $\mu > 0$, $\nu < 0$, $0 < p \leq 2$, $q \geq 2$ in Fig. 1(b) is $\mu = 2$, $\nu = -0.1$, $p = 1.2$, $q = 2.3$.

To compare the computational performance of these systems more comprehensively, for different problem sizes of m, some comparison results are reported in Table 1. From the horizontal view of this table, as the scale of absolute value equations increases, the tracking errors of the system (3.8) in [23] and IFDS with $\mu = 2$, $\nu = -0.1$, $p = 1.2$, $q = 2.3$ are almost unchanged, which shows that they can effectively solve some large-scale problems without increasing the errors to a certain extent. Furthermore, from the vertical view of Table 1, it can be seen that the calculation accuracy of our systems is higher than that of the system (3.8) in [23], and the tracking error of IFDS with $\mu = 0.4$, $\nu = 1$, $p = 7.2$, and $q = 0.5$ is the best among these systems.

From Example 1, it can be seen that the three dynamical systems quickly converge to the solution of AVE (1.1) and their calculation accuracy is acceptable in most cases. As the scale of Example 1 increases, the tracking errors of all dynamical systems are almost unchanged, which shows that they can effectively solve some large-scale problems. It should be noticed that IFDS with $\mu = 0.4$, $\nu = 1$, $p = 7.2$, $q = 0.5$ and IFDS with $\mu = 2$, $\nu = -0.1$, $p = 1.2$, $q = 2.3$ are better than the system (3.8) in [23] in terms of the convergence speed and tracking error. Different from the system (3.8) in [23], we can flexibly select the parameters in IFDS to achieve efficient computation. Moreover, among these dynamical system, our systems have the best computation accuracy, especially for the high-dimensional AVEs. This indicates our systems are effective and have advantages in addressing the AVEs.

6. Conclusions

In this paper, a new inverse-free dynamical system was proposed to solve AVE (1.1). Meanwhile, a tighter global error bound for AVE (1.1) was obtained. As demonstrated, the proposed dynamical system converges the solution to AVE (1.1). Moreover, the proposed dynamical system with concise structure was proved to be globally sublinear and exponential convergent under some suitable conditions on the designed parameters. The simulations verify the correctness of our theoretical results.

Acknowledgments
The first author was supported by the Project of Mathematics and Finance Research Center of Dazhou (SCMF202206), and Natural Science Research General Project for Sichuan University of Arts and Sciences of China (2017KZ010Y). The third author was supported by the National Natural Science Foundation of China (12071379, 11401487), Natural Science Foundation of Chongqing (cstc2021jcyj-msxmX0925, cstc2022ycjh-bgzxm0097), and Education Committee Project Research Foundation of Chongqing (KJQN202201802). The forth author was supported by the Natural Science Foundation of Sichuan Province (2023NSFSC1433).

References

[1] O.L. Mangasarian, R.R. Meyer, Absolute value equations, Linear Algebra Appl. 419 (2006), 359-367.
[2] T. Huang, M. Li, X. Qin, W. Zhu, A CNN-based policy for optimizing continuous action control by learning state sequences, Neurocomputing, 468 (2022), 286-295.
[3] B. He, Inexact implicit methods for monotone general variational inequalities, Math. Program. 86 (1999), 199-217.
[4] B. Tan, X. Qin, S.Y. Cho, Revisiting subgradient extragradient methods for solving variational inequalities, Numer. Algor. 90 (2022), 1593-1615.
[5] R. Li, Local gap density for clustering high-dimensional data with varying densities, Knowledge-Based Syst. 184 (2019), 104905.
[6] N.T. An, P.D. Dong, X. Qin, Robust feature selection via nonconvex sparsity-based methods, J. Nonlinear Var. Anal. 5 (2021), 59-77.
[7] S. Wu, P. Guo, On the unique solvability of the absolute value equation, J. Optim. Theory Appl. 169 (2016), 705-712.
[8] M. Zamani, M. Hladík, Error bounds and a condition number for the absolute value equations, Math. Program. 198 (2023), 85-113.

[9] C. Zhang, Q. Wei, Global and finite convergence of a generalized Newton method for absolute value equations, J. Optim. Theory Appl. 143 (2009), 391-403.
[10] C. Li, A modified generalized Newton method for absolute value equations, J. Optim. Theory Appl. 170 (2016), 1055-1059.
[11] Y.-F. Ke, C.-F. Ma, SOR-like iteration method for solving absolute value equations, Appl. Math. Comput. 311 (2017), 195-202.
[12] X. Dong, X.-H. Shao, H.-L. Shen, A new SOR-like method for solving absolute value equations, Appl. Numer. Math. 156 (2020), 410-421.
[13] L. Xiao, Y. Zhang, Z. Hu, J. Dai, Performance benefits of robust nonlinear zeroing neural network for finding accurate solution of Lyapunov equation in presence of various noises, IEEE Trans. Ind. Inf. 15 (2019), 5161-5171.
[14] M.-F. Leung, J. Wang, Minimax and biobjective portfolio selection based on collaborative neurodynamic optimization, IEEE Trans. Neural Netw. Learn. Syst. 32 (2021), 2825-2836.
[15] X. Ju, D. Hu, C. Li, X. He, G. Feng, A novel fixed-time converging neurodynamic approach to mixed variational inequalities and applications, IEEE Trans. Cybern. 52 (2022), 12942-12953.
[16] E.R. Csetnek, Y. Malitsky, M. K. Tam, Shadow Douglas-Rachford splitting for monotone inclusions, Appl. Math. Optim. 80 (2019), 665-678.
[17] X. Han, X. He, X. Ju, A distributed neurodynamic algorithm for sparse signal reconstruction via ℓ_1-minimization, Neurocomputing, doi: https://doi.org/10.1016/j.neucom.2023.126480.
[18] Y. Xia, J. Wang, A bi-projection neural network for solving constrained quadratic optimization problems, IEEE Trans. Neural Netw. Learn. Syst. 27 (2016), 214-224.
[19] A. Mansoori, M. Eshaghnezhad, S. Effati, An efficient neural network model for solving the absolute value equations, IEEE Trans. Circuits Syst. II Exp. Briefs 65 (2018), 391-395.
[20] A. Mansoori, M. Erfanian, A dynamic model to solve the absolute value equations, J. Comput. Appl. Math. 333 (2018), 28-35.
[21] B. Saheya, C.T. Nguyen, J.S. Chen, Neural network based on systematically generated smoothing functions for absolute value equation, J. Appl. Math. Comput. 61 (2019), 533-558.
[22] X. Ju, C. Li, X. Han, X. He, Neurodynamic network for absolute value equations: A fixed-time convergence technique, IEEE Trans. Circuits Syst. II Exp. Briefs 69 (2022), 1807-1811.
[23] C. Chen, Y. Yang, D. Yu, D. Han, An inverse-free dynamical system for solving the absolute value equations, Appl. Numer. Math. 168 (2021), 170-181.
[24] D. Yu, C. Chen, Y. Yang, D. Han, An inertial inverse-free dynamical system for solving absolute value equations, J. Ind. Manag. Optim. 19 (2023), 2549-2559.
[25] J. Xu, X. He, X. Han, H. Wen, A two-layer distributed algorithm using neurodynamic system for solving L_1-minimization, IEEE Trans. Circuits Syst. II Exp. Briefs 69 (2022), 3490-3494.
[26] H.K. Khalil, Nonlinear Systems (3rd ed.), Upper Saddle River, New Jersey: Prentice-Hall, 2002.
[27] M. Firouzbahrami, A. Nobakhti, Cooperative fixed-time/finite-time distributed robust optimization of multi-agent systems, Automatica 142 (2022), 110358.
[28] R.A. Horn, C.R. Johnson, Matrix Analysis, Cambridge University Press, Cambridge, 2013.
[29] C.R. Johnson, Multiplicativity and compatibility of generalized matrix norms, Linear Algebra Appl. 16 (1977), 25-37.
[30] Y. Hu, C. Li, K. Meng, J. Qin, X. Yang, Group sparse optimization via lp,q regularization, J. Mach. Learn. Res. 18 (2017), 960-1011.
[31] P. Guo, S. Wu, C. Li, On the SOR-like iteration method for solving absolute value equations, Appl. Math. Lett. 97 (2019), 107-113.